Chapter 3

Background Knowledge

The biomechanical modeling of biological structures requires a comprehensive knowledge of the following major fields of study

- anatomy,
- continuum mechanics,
- numerical mathematics, in particular, the finite element method.

This chapter is ordered in three major sections, which cover the basics of these disciplines and contain issues relevant to the numerical modeling of deformable facial tissue.

3.1 Facial Tissue. Structure and Properties

In this section, we make a brief overview of anatomy and biophysics of facial tissues with emphasis on their passive mechanical properties. Biomechanics of muscle contraction will be discussed separately, in Chapter 7.

Anatomy. Soft tissue is a collective term for almost all anatomical structures, which can be named soft in comparison to bones. In this work, we focus on biomechanical modeling of facial tissue only.

Soft tissues are mainly composed of different types of polymeric molecules embedded in a hydrophilic gel called ground substance [44]. A basic structural element of facial and other soft tissues is collagen, which amounts up to 75% of dry weight. The remaining weight is shared between elastin, actin, reticulin and other polymeric proteins. Biopolymers are organized in hierarchical bundles

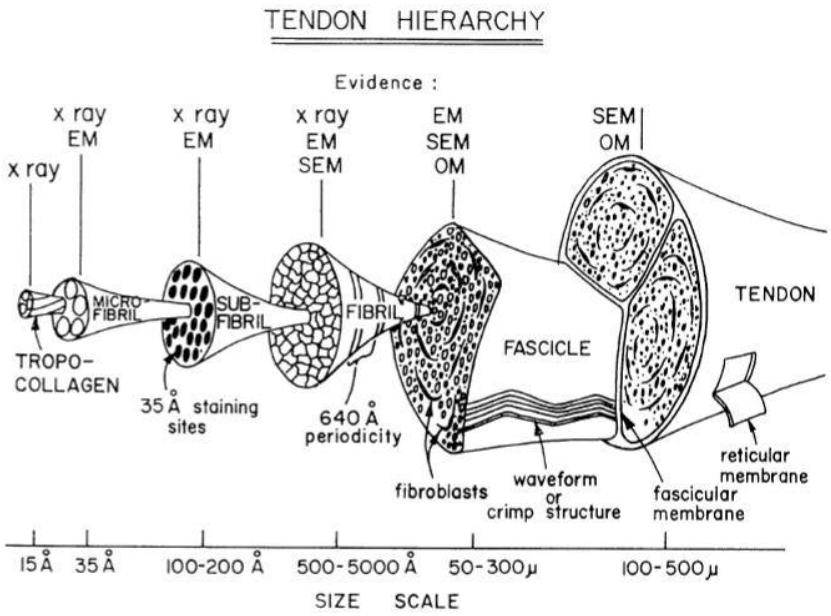

Figure 3.1: Hierarchical organization of fibrous structures in tendon (from [44]).

of fibers arranged in a more or less parallel fashion in the direction of the effort handled [85], see Figure 3.1.

The direction of collageneous bundles (connective tissue) in the skin determines lines of tension, the so-called *Langer's Lines* [28], see Figure 3.2. The

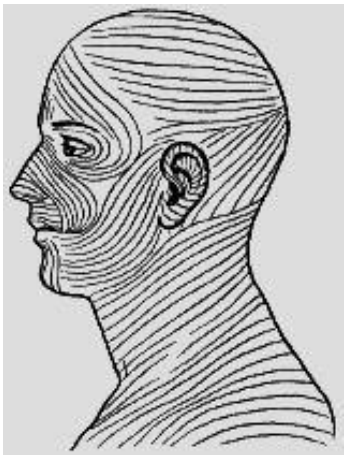

Figure 3.2: Langer's lines (from [62]).

arrangement of fibrous structures in the skin is individual, which, in particular, reflects in the individual wrinkles of the skin. Generally, the fiber networks of different tissues are composed of both irregular and ordered regions. In muscles and tendons, fibers are arranged in orderly patterns (cf. Figure 3.1), whereas fibers in connective tissue are arranged more randomly.

Further, facial tissue consists of the following anatomically and microbiologically distinctive layers:

- skin
  - epidermis
  - dermis
- subcutis (hypodermis)
- fascia
- muscles

In Figure 3.3, a typical cross-section of facial tissue (left) and the corresponding discrete layer model (right) are shown. The skin consists of two biaxial layers:

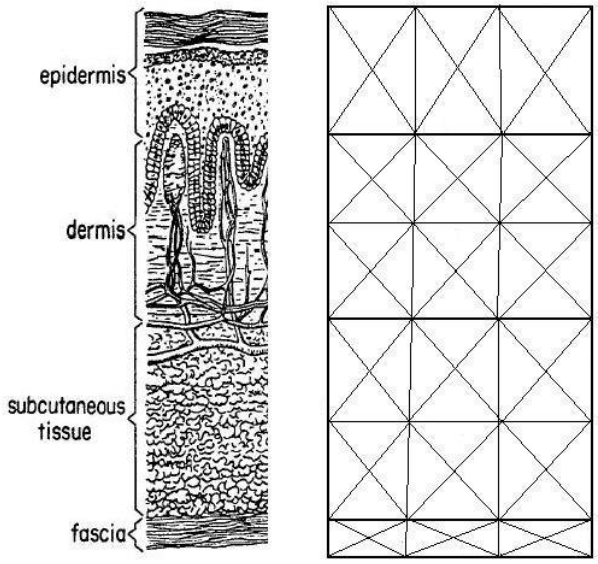

Figure 3.3: Left: skin cross-section (from [85]). Right: the corresponding discrete layer model.

a comparatively thin layer of stratified epithelium, called epidermis and a thicker dermis layer. The dermis layer contains disordered collagen and elastin fibers embedded in the gelatinous ground substance. The thickness of the skin varies between 1.5mm and 4mm. The dermis layer of the skin is continuously connected by collagen fibers to a subcutaneous fatty tissue, called the hypodermis. In turn, the hypodermis is connected to the fibrous fascia layer, which surrounds the muscle bundles. The contact between the lower subcutaneous tissue layer and the muscle fascia is flexible, which appears as a kind of sliding between the skin and other internal soft tissues.

Biomechanics. *Biomechanics* combines the field of engineering mechanics with the fields of biology and physiology and is concerned with the analysis of mechanical principles of the human body. While studying the living tissue biomechanics, the common practice has always been to utilize the engineering methods and models known from "classic" material science. However, the living tissues have properties that make them very different from normal engineering materials. The first important fact is that all living tissues are open thermodynamic systems. Living organisms permanently consume energy and exchange matter with their environment to maintain the essential metabolic processes. For example, living tissues have *self-adapting* and *self-repairing* abilities, which enable wound healing and stress relaxation of loaded tissue.

Numerous experimental and theoretical studies in the field of tissue biomechanics have been carried out in recent years [44, 85, 90, 7]. Summarizing the facts observed in different experiments with different tissue types, soft tissues generally exhibit *non-homogeneous, anisotropic, quasi-incompressible, non-linear plastic-viscoelastic* material properties, which we briefly describe hereafter.

Non-homogeneity, anisotropy. Soft tissues are multi-composite materials containing cells, intracellular matrix, fibrous and other microscopical structures. This means that the mechanical properties of living tissues vary from point to point within the tissue. Essential for modeling are the spatial distribution of material stiffness and the organization of fibrous structures such as collagen and elastin fibers, which have some preferential orientation in the skin. The dependence on coordinates along the same spatial direction is called non-homogeneity. If a material property depends on the direction, such material is called anisotropic. Facial tissue is both non-homogeneous and anisotropic. However, there are practically no quantitative data about these properties and thus their importance for modeling of relatively thin facial tissue is uncertain.

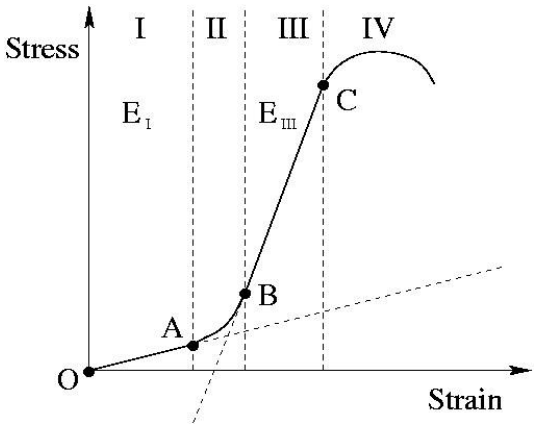

Figure 3.4: Non-linear stress-strain curve of soft tissue (from [44, 90]).

Non-linearity. The stress-strain relationship, the so-called *constitutive equation* of the skin and other soft tissues is non-linear [70]. The non-linear stress-strain curve, shown in Figure 3.4, is usually divided in four phases. At low strains (phase I: $\varepsilon < \varepsilon_A$), the response of soft tissue is linear; at average strains (phase II: $\varepsilon_A \leq \varepsilon < \varepsilon_B$), the straightening of collagen fibers occurs and the tissue stiffness increases; at high strains (phase III: $\varepsilon_B \leq \varepsilon < \varepsilon_C$), all fibers are straight and the stress-strain relationship becomes linear again. By larger strains (phase IV: $\varepsilon > \varepsilon_C$), material destruction occurs. The phase II is often neglected and the stress-strain curve is considered piecewise linear. There are no quantitative data about the stiffness coefficients E_{I-III} and the critical strains $\varepsilon_{A,B,C}$ for the bilinear approximation of facial tissue. However, it is observed that these parameters depend on different factors and may vary from person to person. For instance, the critical strain ε_C decreases with age [85].

Plasticity. The deformation of physical bodies is reversible in the range of small strains only. Large deformations lead to irreversible destruction of material, which appears as a cyclic stress-strain curve that shows the basic difference of material response in loading and unloading, i.e., the so-called hysteresis loop, see Figure 3.5. Such deformations are called plastic in a difference to the reversible elastic deformations. It is reasonable to assume that soft tissue exhibits plastic behavior up to some critical strain as every known engineering material. However, living tissues possess the self-reparing ability, which means that after a certain period of time the destructive alterations are reversed by repairing mechanisms. Obviously, the "factor time" is essential for the choice of an appropriate material model of soft tissue biomechanics. Within a comparatively short period of time (immedi-

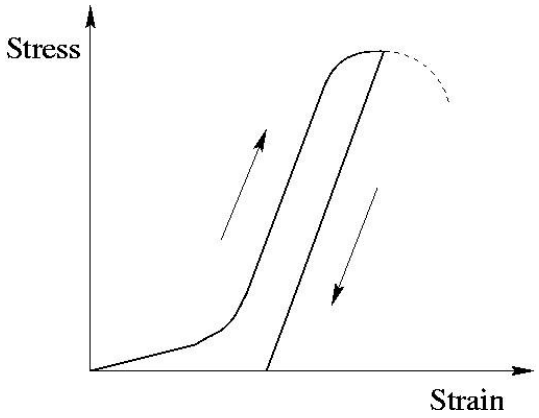

Figure 3.5: Hysteresis loop for an elasto-plastic material (from [90]).

ately after the destructive impact), soft tissue behaves as every "normal material". However, even massive destructions completely disappear without any markable irreversible alterations after several days or weeks of healing. At present, too little is known about the plastic behavior of living tissues to estimate its relevancy for the modeling of the quasi-static deformations.

Viscoelasticity. The time-dependent material behavior is called viscoelasticity. The response of such materials depends on the history of the deformation, that is the stress $\sigma = \sigma(\varepsilon, \varepsilon')$ is a function of both the strain ε and the strain rate $\varepsilon' = d\varepsilon/dt$, where t is the time. Viscosity is originally a fluid property. Elasticity is a property of solid materials. Therefore, a viscoelastic material combines both fluid and solid properties. Soft tissue, for example the skin, exhibits properties that can be interpreted as viscoelastic. Two characteristics of tissue time-dependent behavior are *creep* and *stress relaxation* or *recovery*. Both creep and recovery can be explained by observing the material response to a constant stress σ_0 applied at time t_0 and removed at time t_1. The responses of a linear elastic solid, a viscoelastic solid and a viscoelastic fluid are shown in Figure 3.6. A linear elastic material shows an immediate response and completely recovers the deformation after the loading is removed, see Figure 3.6 (b). A viscoelastic material responds with an exponentially increasing strain $\varepsilon \sim (1 - exp(-t/\tau_1))$ between times t_0 and t_1. After the loading is removed, at time t_1, an exponential recovery $\varepsilon \sim exp(-t/\tau_1)$ begins. A viscoelastic solid will completely recover, see Figure 3.6 (d). For a viscoelastic fluid, see Figure 3.6 (c), a residual strain will remain in the material and complete recovery will never be achieved. The characteristic time τ of the exponential recovery curve $\varepsilon \sim \exp(-t/\tau)$ of soft tissue lies between milliseconds and seconds [44, 68]. Since soft tissue does not exhibit long time memory, the vis-

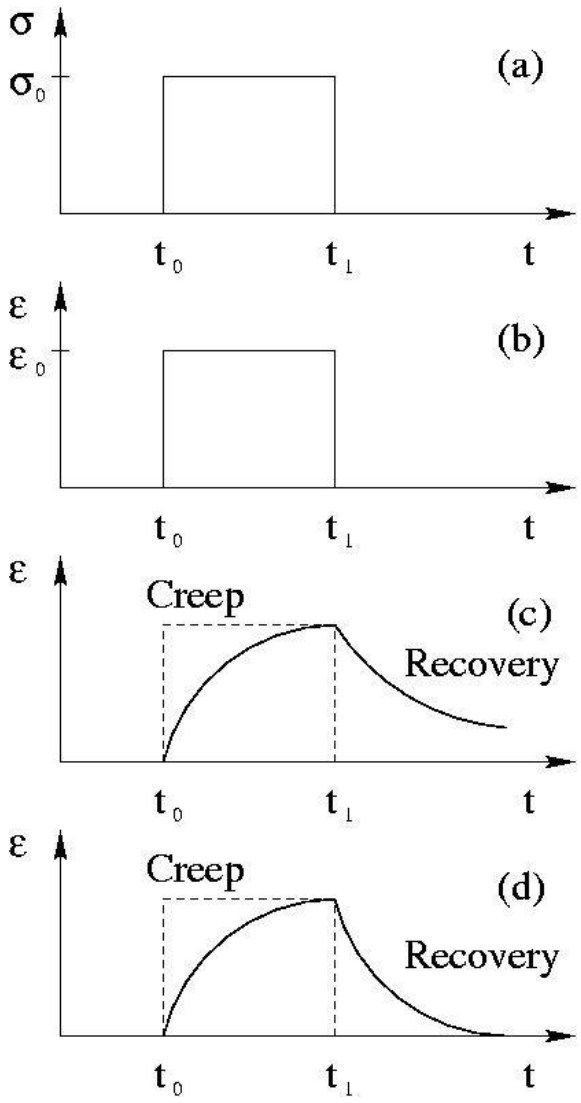

Figure 3.6: Creep and recovery (from [90]). (a): constant stress σ_0 applied at time t_0 and removed at time t_1. (b): response of a linear elastic material. (c): response of a viscoelastic fluid. (d): response of a viscoelastic solid.

coelastic phenomena can be assumed neglectable for the "long term" prediction, i.e., $t \gg \tau_{\text{max}} = 10\,s$.

Quasi-incompressible material. A material is called incompressible if its volume remains unchanged by the deformation. Soft tissue is a composite material that consists of both incompressible and compressible ingredients. Tissues with high proportion of water, for instance the brain or water-rich parenchymal organs are usually modeled as incompressible materials, while tissues with low water proportion are assumed quasi-incompressible. In this works, we describe facial tissue as a quasi-incompressible material. Further discussion of the constitutive model of soft tissue is in Chapter 5.

In Table 3.1, the material properties of soft tissue in conjunction with their relevancy for the modeling of quasi-static facial tissue are summarized. Comprising this information, facial tissue can be approximated as a *piecewise homogeneous, isotropic, quasi-incompressible non-linear elastic* solid.

Table 3.1: Relevancy of general material properties for quasi-static facial tissue modeling.

Property	Relevancy remarks
non-homogeneity	piecewise homogeneous approximation assumed
anisotropy	isotropic approximation assumed
non-linear elasticity	basic continuum property
plasticity	short term prediction and large deformations only
viscosity	short term prediction only
compressibility	quasi-incompressible approximation assumed

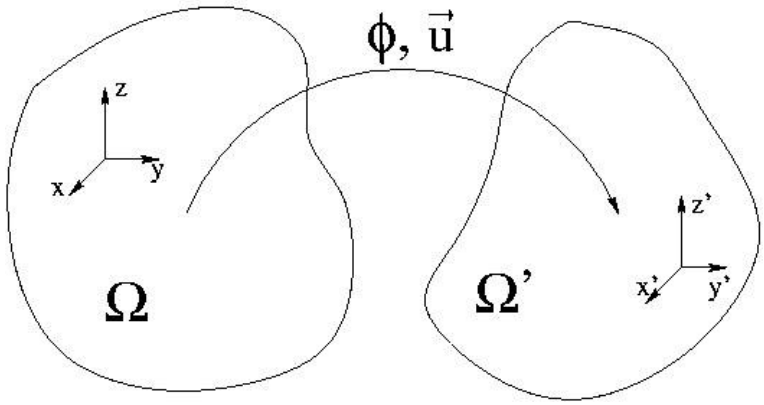

Figure 3.7: 3D domain deformation.

3.2 Basics of Continuum Mechanics

In this section, we describe the basic mathematical definitions of elasticity theory. In elasticity theory, physical bodies are described as continua. Under the impact of external forces, physical bodies are deformed, which means that they change both their shape and volume. Let $\Omega \subset \mathbb{R}^3$ be a domain representing the volume occupied by a body before the deformation. The state of a body associated with such "undeformed" domain is called the *reference configuration*.

Deformations. A *deformation* of the reference configuration Ω with Lipschitz-continuous boundary Γ is defined by a smooth orientation-preserving vector field

$$\boldsymbol{\phi} : \Omega \rightarrow \mathbb{R}^3 , \tag{3.1}$$

which maps the reference configuration onto the *deformed configuration* $\Omega' = \boldsymbol{\phi}(\Omega)$, see Figure 3.7. Further, we define the *deformation gradient* as a matrix

$$\boldsymbol{\nabla\phi} = \begin{pmatrix} \partial_1\phi_1 & \partial_2\phi_1 & \partial_3\phi_1 \\ \partial_1\phi_2 & \partial_2\phi_2 & \partial_3\phi_2 \\ \partial_1\phi_3 & \partial_2\phi_3 & \partial_3\phi_3 \end{pmatrix}, \tag{3.2}$$

where $\partial_k = \partial/\partial x_k$. The orientation-preserving condition for the deformation is given by

$$\det(\boldsymbol{\nabla\phi}) > 0. \tag{3.3}$$

Displacements. For practical reasons, it is often convenient to use the displacement field (*displacements*) $\mathbf{u} : \Omega \to \mathbb{R}^3$ instead of the deformation field $\boldsymbol{\phi}$

$$\mathbf{u} = \boldsymbol{\phi}(\mathbf{x}) - \mathbf{x} = \mathbf{x}' - \mathbf{x}\,, \tag{3.4}$$

where $\mathbf{x} \in \boldsymbol{\Omega}$ and $\mathbf{x}' \in \boldsymbol{\Omega}'$ denote the coordinates of the same point in the reference and deformed configuration, respectively. Variables defined as a function of coordinates in the reference configuration $\mathbf{x}$ are called *Lagrange* variables and those of coordinates in the deformed configuration $\mathbf{x}'$ are called *Euler* variables. Analogously to (3.2), the *displacement gradient* is defined

$$\boldsymbol{\nabla}\mathbf{u} = \begin{pmatrix} \partial_1 u_1 & \partial_2 u_1 & \partial_3 u_1 \\ \partial_1 u_2 & \partial_2 u_2 & \partial_3 u_2 \\ \partial_1 u_3 & \partial_2 u_3 & \partial_3 u_3 \end{pmatrix} \tag{3.5}$$

and (3.3) can be re-written as

$$\det(\mathbf{I} + \boldsymbol{\nabla}\mathbf{u}) > 0. \tag{3.6}$$

Strain tensor. Consider an infinitesimal distance between two points $P(\mathbf{x})$ and $P'(\mathbf{x} + \mathbf{dx})$. The square of an Euclidian infinitesimal distance in the reference configuration is given by

$$ds^2 = d\mathbf{x}^{\mathrm{T}} d\mathbf{x}\,. \tag{3.7}$$

The square of an infinitesimal distance in the deformed configuration can be similarly written as

$$ds'^2 = d\mathbf{x}'^{\mathrm{T}} d\mathbf{x}'\,. \tag{3.8}$$

Recalling that

$$d\mathbf{x}' = \boldsymbol{\nabla}\boldsymbol{\phi}\, d\mathbf{x} \tag{3.9}$$

(3.8) can be re-written in terms of the reference configuration

$$ds'^2 = d\mathbf{x}^{\mathrm{T}}\, \boldsymbol{\nabla}\boldsymbol{\phi}^{\mathrm{T}} \boldsymbol{\nabla}\boldsymbol{\phi}\, d\mathbf{x} = d\mathbf{x}^{\mathrm{T}} \mathbf{C} d\mathbf{x}\,, \tag{3.10}$$

where $\mathbf{C} = \boldsymbol{\nabla}\boldsymbol{\phi}^{\mathrm{T}} \boldsymbol{\nabla}\boldsymbol{\phi}$ denotes the *Cauchy-Green strain tensor*. With $\boldsymbol{\phi} = \mathbf{x} + \mathbf{u}$ we can write

$$\mathbf{C} = \boldsymbol{\nabla}\boldsymbol{\phi}^{\mathrm{T}} \boldsymbol{\nabla}\boldsymbol{\phi} = \mathbf{I} + \boldsymbol{\nabla}\mathbf{u}^{\mathrm{T}} + \boldsymbol{\nabla}\mathbf{u} + \boldsymbol{\nabla}\mathbf{u}^{\mathrm{T}}\, \boldsymbol{\nabla}\mathbf{u}\,. \tag{3.11}$$

The deviation from the identity in (3.11) is the *Green-St. Venant strain tensor* or simply the strain tensor $\boldsymbol{\varepsilon}$

$$\boldsymbol{\varepsilon}(\mathbf{u}) = \frac{1}{2}\left(\mathbf{C} - \mathbf{I}\right) = \frac{1}{2}\left(\boldsymbol{\nabla}\mathbf{u}^{\mathrm{T}} + \boldsymbol{\nabla}\mathbf{u} + \boldsymbol{\nabla}\mathbf{u}^{\mathrm{T}}\boldsymbol{\nabla}\mathbf{u}\right) \tag{3.12}$$

or componentwise under consideration of Einstein's sum notation

$$\varepsilon_{ij} = \frac{1}{2}(\partial_j u_i + \partial_i u_j + \partial_i u_l \partial_j u_l)\,. \tag{3.13}$$

Since the strain tensor is obviously symmetric, i.e., $\varepsilon_{ij} = \varepsilon_{ji}$, there is a coordinate system called *principal axes of the tensor*, where it only has diagonal non-zero components $(\varepsilon^I, \varepsilon^{II}, \varepsilon^{III})$. Such principal axes transformation is local and generally holds for an infinitesimal surrounding of the point $P(\mathbf{x})$ only. In principal axes, the infinitesimal distance (3.10) can be written

$$ds'^2 = (1 + 2\varepsilon^I)dx_1'^2 + (1 + 2\varepsilon^{II})dx_2'^2 + (1 + 2\varepsilon^{III})dx_3'^2\,, \tag{3.14}$$

which means that every local deformation can be represented as a superposition of three independent strains along the orthogonal principal axes

$$\frac{dx_i'}{dx_i} = \sqrt{1 + 2\varepsilon^i}\,. \tag{3.15}$$

Thus, the expressions $\sqrt{1 + 2\varepsilon^i}$ represent the elongation of the i-th principal axis. In the case of small deformations, the relative elongations are small in comparison with 1, i.e., $\varepsilon^i \ll 1$ and are given by

$$\frac{dx_i' - dx_i}{dx_i} = \sqrt{1 + 2\varepsilon^i} - 1 \approx \varepsilon^i\,. \tag{3.16}$$

We then consider an infinitesimal volume around the point $P(\mathbf{x})$, which is given by $dV' = dx_1' dx_2' dx_3'$ in the deformed configuration and by $dV = dx_1 dx_2 dx_3$ in the reference configuration, respectively. Under consideration of (3.16), the differential quotient dV'/dV, which indicates the variation of an infinitesimal volume by the deformation, is given by

$$\frac{dV'}{dV} = (1 + \varepsilon^I)(1 + \varepsilon^{II})(1 + \varepsilon^{III}) \approx (1 + \varepsilon^I + \varepsilon^{II} + \varepsilon^{III})\,. \tag{3.17}$$

The sum of eigenvalues $\varepsilon^I + \varepsilon^{II} + \varepsilon^{III}$ is an invariant of the strain tensor $\boldsymbol{\varepsilon}$, which does not depend on the coordinate system and is generally given by the sum of the diagonal components of $\boldsymbol{\varepsilon}$. (3.17) can be re-written as follows

$$\frac{dV' - dV}{dV} = \mathrm{tr}(\boldsymbol{\varepsilon})\,, \tag{3.18}$$

where $\mathrm{tr}(\boldsymbol{\varepsilon}) = \varepsilon_{ll}$. Thus, the trace of $\boldsymbol{\varepsilon}$ describes the relative volume difference by the deformation. In the case of volume preserving deformations, for example by incompressible materials, the trace of the strain tensor vanishes, $\mathrm{tr}(\boldsymbol{\varepsilon}) = 0$.

Generally, the strain can be represented as a sum of *pure shearing* and *homogeneous dilatation*. The corresponding terms of the strain tensor are called the *deviatoric* (subscript d) and *volumetric* or *mean* component (subscript m) and are given by

$$\begin{aligned} \boldsymbol{\varepsilon} &= \boldsymbol{\varepsilon}_d + \boldsymbol{\varepsilon}_m \,, \\ \boldsymbol{\varepsilon}_d &= \boldsymbol{\varepsilon} - \tfrac{1}{3}\mathrm{tr}(\boldsymbol{\varepsilon})\,\mathbf{I}\,, \\ \boldsymbol{\varepsilon}_m &= \tfrac{1}{3}\mathrm{tr}(\boldsymbol{\varepsilon})\,\mathbf{I}\,. \end{aligned} \tag{3.19}$$

Geometrical non-linearity. The mapping $\mathbf{u} \to \boldsymbol{\varepsilon}$ is generally non-linear, cf. (3.12). This fact is known as *geometrical non-linearity*. In the case of small deformations, the maximal eigenvalue of the strain tensor ε^i, which represents the maximal elongation of the principle axes, is *signifi cantly smaller*than 1

$$\epsilon = \max(|\varepsilon^i|) \ll 1\,. \tag{3.20}$$

In this case, the quadratic term in (3.12) can be neglected and the strain tensor can be linearized

$$\boldsymbol{\varepsilon}(\mathbf{u}) \approx \mathbf{e}(\mathbf{u}) = \frac{1}{2}(\boldsymbol{\nabla}\mathbf{u}^{\mathrm{T}} + \boldsymbol{\nabla}\mathbf{u})\,. \tag{3.21}$$

For the monitoring of the local linearization error, (3.20) can be used in a more exact form

$$\epsilon = \max(|e^i|) < \epsilon_{max}\,, \tag{3.22}$$

where e^i are the eigenvalues of the gradient matrix $\boldsymbol{\nabla}\mathbf{u}$ and ϵ_{max} denotes a typical threshold for the maximum relative linearization error of approximately three percent, i.e., $\epsilon_{max} = 0.03$.

Stress tensor. Consider a physical body occupying the deformed confi guration Ω'. The forces that cause the deformation are called *external* forces. Under the impact of external forces $\mathbf{F'}_{\mathrm{ex}}$ *internal* forces (*stresses*) $\mathbf{F'}_{\mathrm{in}}$ arise. Generally, external forces can act inside the deformed domain $\mathbf{F'}_{\mathrm{ex}} : \Omega' \to \mathbb{R}^3$ (applied body forces) or on its boundary $\mathbf{G'}_{\mathrm{ex}} : \Gamma' \to \mathbb{R}^3$ (applied surface forces). In accordance with *Euler-Cauchy stress principle*, there exists the vector $\mathbf{t}' : \boldsymbol{\Omega}' \to \mathbb{R}^{\mathbf{3}}$ (the *Cauchy*

stress vector or *traction*) such that: for any subdomain V' of Ω' and any point of its boundary $\mathbf{x}' \in \mathbf{S}' \cap \partial V'$

$$\mathbf{F}'_{\text{in}} = \int_{\partial V'} \mathbf{t}'(\mathbf{x}', \mathbf{n}')\, dS' \,, \tag{3.23}$$

where $\mathbf{n}'$ is the unit outer normal vector to $\partial V'$. Furthermore, according to *Cauchy' theorem* there exists the symmetric tensor of rank 2 (*Cauchy stress tensor*) $\mathbf{T}' : \Omega' \to \mathbb{R}^{3\times 3}$ such that

$$\mathbf{t}'(\mathbf{x}', \mathbf{n}') = \mathbf{T}'(\mathbf{x}')\mathbf{n}' \,. \tag{3.24}$$

Static equilibrium state. In static equilibrium, the sum of external and internal forces vanish

$$\mathbf{F}'_{\text{ex}} + \mathbf{F}'_{\text{in}} = 0 \,. \tag{3.25}$$

By applying the *Gauss theorem* [42] to (3.23) and (3.24) one obtains

$$\mathbf{F}'_{\text{in}} = \int_{\partial V'} \mathbf{T}'(\mathbf{x}')\mathbf{n}'\, dS' \; = \int_{\Omega'} \text{div}\mathbf{T}'(\mathbf{x}')\, dV' \,. \tag{3.26}$$

If $\mathbf{f}'(\mathbf{x}')$ denotes the density of external forces in the deformed configuration

$$\mathbf{F}'_{\text{ex}} = \int_{\Omega'} \mathbf{f}'(\mathbf{x}') dV' \tag{3.27}$$

the equation of static equilibrium (3.25) can be written as

$$\int_{\Omega'} \mathbf{f}'(\mathbf{x}') dV' + \int_{\Omega'} \text{div}\mathbf{T}'(\mathbf{x}')\, dV' = 0 \tag{3.28}$$

or in differential form

$$-\text{div}\mathbf{T}'(\mathbf{x}') = \mathbf{f}'(\mathbf{x}'). \tag{3.29}$$

(3.29) describes the static equilibrium for an infinitesimal volume element in the deformed configuration. With the help of *Piola transformation* one can obtain an analogous formulation in the reference configuration

$$-\text{div}\mathbf{T}(\mathbf{x}) = \mathbf{f}(\mathbf{x}), \tag{3.30}$$

where $\mathbf{T}(\mathbf{x}) = \det(\boldsymbol{\nabla}\boldsymbol{\phi})\mathbf{T}'(\mathbf{x}')\boldsymbol{\nabla}\boldsymbol{\phi}^{-\mathrm{T}}$ is the *first Piola-Kirchhoff stress tensor* and $\mathbf{f}(\mathbf{x})$ denotes the density of external forces in the reference configuration. Instead of the first Piola-Kirchhoff stress tensor, we will use the symmetric *second Piola-Kirchhoff stress tensor* or simply the stress tensor

$$\boldsymbol{\sigma}(\mathbf{x}) = \boldsymbol{\nabla}\boldsymbol{\phi}^{-1}\mathbf{T}(\mathbf{x})\,, \tag{3.31}$$

which is directly related to constitutive equations. By setting (3.31) in (3.30) one obtains the equation of the static equilibrium in the reference configuration (*Lagrange formulation*) in respect to $\boldsymbol{\sigma}$

$$-\mathrm{div}\,\{(\mathbf{I}+\boldsymbol{\nabla}\mathbf{u})\,\boldsymbol{\sigma}(\mathbf{x})\} = \mathbf{f}(\mathbf{x}). \tag{3.32}$$

Constitutive equation. In continuum mechanics, material properties are described by the so-called *response function*, which implies the strain-stress relationship (*constitutive equation*), or by the *stored energy function*. The correct modeling of material properties is a challenging task studied within the scope of materials science. Though, some special energy functionals for living tissues were proposed in the past [28, 44, 61], no established and extensive investigations have yet been reported, which would underlay the advantages of one constitutive model of soft tissue over the others. Taking into account that the strain-stress relationship for soft tissue can be approximated by a bilinear function (see Section 3.1), a constitutive model of soft tissue based on the piecewise linear stress-strain relationship seems to be a reasonable approximation. Generally, the linear relationship between two tensors of rank 2 is given by the tensor of rank 4

$$\boldsymbol{\sigma}(\boldsymbol{\varepsilon}) = \mathrm{C}\,\boldsymbol{\varepsilon}\,. \tag{3.33}$$

In respect to the strain-stress relationship (3.33), the tensor C is called the *tensor of elastic constants* and the constitutive equation (3.33) is known as the *generalized Hook's law*.

St. Venant-Kirchhoff material. Under consideration of the *frame-indifference*, i.e., the invariance under coordinate transformations, the tensor of elastic constants C for *isotropic* and *homogeneous* materials contains only two independent constants and (3.33) can be written in explicit form

$$\boldsymbol{\sigma}(\boldsymbol{\varepsilon}) = \lambda\mathrm{tr}(\boldsymbol{\varepsilon})\mathbf{I} + 2\mu\boldsymbol{\varepsilon}\,. \tag{3.34}$$

A material described by the constitutive equation (3.34) is called a *St. Venant-Kirchhoff* material. Although the mapping $\boldsymbol{\varepsilon} \rightarrow \boldsymbol{\sigma}(\boldsymbol{\varepsilon})$ for a St. Venant-Kirchhoff

material is linear, the associated mapping $\mathbf{u} \rightarrow \boldsymbol{\sigma}(\boldsymbol{\varepsilon}(\mathbf{u}))$ is due to the non-linearity of the strain tensor basically non-linear

$$\boldsymbol{\sigma}(\boldsymbol{\varepsilon}(\mathbf{u})) = \lambda(\mathrm{tr}\boldsymbol{\nabla}\mathbf{u})\mathbf{I} + \mu(\boldsymbol{\nabla}\mathbf{u}^{\mathrm{T}} + \boldsymbol{\nabla}\mathbf{u}) + \frac{\lambda}{2}(\mathrm{tr}\boldsymbol{\nabla}\mathbf{u}^{\mathrm{T}}\boldsymbol{\nabla}\mathbf{u})\mathbf{I} + \mu\boldsymbol{\nabla}\mathbf{u}^{\mathrm{T}}\boldsymbol{\nabla}\mathbf{u}\,. \quad (3.35)$$

The two positive constants in (3.34)

$$\lambda > 0 \text{ and } \mu > 0 \quad (3.36)$$

are the so-called *Lamé constants* [1]. Besides the Lamé constants, another two elastic constants are widely used in material science. These are the *Young modulus* E, which describes the material stiffness, and the *Poisson ratio* ν, which describes the material compressibility. (λ, μ) and (E, ν) are related by the following equations

$$\begin{aligned} \nu &= \frac{\lambda}{2(\lambda+\mu)}\,, & E &= \frac{\mu(3\lambda+2\mu)}{\lambda+\mu} \\ \lambda &= \frac{E\nu}{(1+\nu)(1-2\nu)}\,, & \mu &= \frac{E}{2(1+\nu)} \end{aligned} \quad (3.37)$$

From (3.36) and (3.37) it follows that

$$0 < \nu < 0.5 \text{ and } E > 0\,. \quad (3.38)$$

With E and ν (3.34) can be re-written as follows

$$\boldsymbol{\sigma}(\boldsymbol{\varepsilon}) = \frac{E}{1+\nu}\left(\frac{\nu}{1-2\nu}\mathrm{tr}(\boldsymbol{\varepsilon})\mathbf{I} + \boldsymbol{\varepsilon}\right). \quad (3.39)$$

Finally, a third alternative form of the constitutive equation is sometimes useful. It represents the relationship between the volumetric and deviatoric components of the stress and the strain, cf. (3.19)

$$\begin{aligned} \boldsymbol{\sigma}_d &= 2G\boldsymbol{\varepsilon}_d\,, \\ \boldsymbol{\sigma}_m &= 3K\boldsymbol{\varepsilon}_m\,, \end{aligned} \quad (3.40)$$

where G denotes the *shear modulus*, which is identical with μ, and $K = \frac{E}{3(1-2\nu)}$ is another elastic constant called the *bulk modulus*.

[1] (3.36) follows from thermodynamic considerations, see [77].

Anisotropic materials. In the case of anisotropic materials, the 9×9 tensor of elastic constants C may generally have a very dense, complex structure. However, if a material has particular planar or axial symmetry, it can be written in a reduced symmetric form. For example, the constitutive equation of an *orthotropic* material, i.e., a material with three mutually perpendicular planes of elastic symmetry, is of the following form

$$\{\sigma\} = \begin{pmatrix} C_{11} & C_{12} & C_{13} & 0 & 0 & 0 \\ C_{12} & C_{22} & C_{23} & 0 & 0 & 0 \\ C_{13} & C_{23} & C_{33} & 0 & 0 & 0 \\ 0 & 0 & 0 & C_{44} & 0 & 0 \\ 0 & 0 & 0 & 0 & C_{55} & 0 \\ 0 & 0 & 0 & 0 & 0 & C_{66} \end{pmatrix} \{\varepsilon\}, \tag{3.41}$$

where

$$\begin{aligned} \{\sigma\}^T &= \{\sigma_{11}, \sigma_{22}, \sigma_{33}, \sigma_{23}, \sigma_{31}, \sigma_{12}\}\,, \\ \{\varepsilon\}^T &= \{\varepsilon_{11}, \varepsilon_{22}, \varepsilon_{33}, 2\varepsilon_{23}, 2\varepsilon_{31}, 2\varepsilon_{12}\}\,. \end{aligned} \tag{3.42}$$

Thus, for modeling an orthotropic material 9 independent constants related to Young moduli E_{ij} and Poisson ratios ν_{ij} in three corresponding space directions are needed. The constitutive equation of a *transversely isotropic* material, i.e., unidirectional fibered material, already contains only5 independent constants [85, 76].

Physical non-linearity. The non-linear strain-stress relationship of soft tissue, which is given by the empiric curve, shown in Figure 3.4, is called the *physical non-linearity*. Reflecting the increasing stiffness of soft tissue with the increasing deformation, this curve can be subdivided into two or more intervals (phases) each one described by the linear strain-stress relationship (3.39). Such a piecewise linear approximation can formally be written as

$$\boldsymbol{\sigma}(\boldsymbol{\varepsilon}(\mathbf{u})) = \mathrm{C}(E^n, \nu)\, \boldsymbol{\varepsilon}(\mathbf{u}) \quad u \in [u^{n-1}, u^n[\,, \tag{3.43}$$

where $u = |\mathbf{u}|$ and E^n denotes the stiffness of n-th linear elastic interval in the range $[u^{n-1}, u^n[$. For the stress-strain curve of soft tissue (cf. Figure 3.4), the bilinear approximation ($n = 2$) with an empirically estimated threshold value of u^1 can be applied.

Hyperelasticity. In elasticity theory, a material is called *hyperelastic*, if there exists a stored energy function $W : \Omega \times \mathbb{M}^3_+ \to \mathbb{R}$ such that

$$\boldsymbol{\sigma}(\boldsymbol{\varepsilon}) = \frac{\partial W}{\partial \boldsymbol{\varepsilon}}\,. \tag{3.44}$$

It can be easily shown that a St. Venant-Kirchhoff material with the response function (3.34) is hyperelastic and its store energy function is given by

$$W(\boldsymbol{\varepsilon}) = \frac{\lambda}{2}(\mathrm{tr}\boldsymbol{\varepsilon})^2 + \mu \mathrm{tr}(\boldsymbol{\varepsilon}^2)\,. \tag{3.45}$$

Boundary conditions. The boundary conditions (BC) arising in the soft tissue modeling are usually given by the prescribed boundary displacements or external forces. Besides the Dirichlet boundary conditions, which in continuum mechanics are better known as the *essential* boundary conditions

$$\mathbf{u}(\mathbf{x}) = \hat{\mathbf{u}}(\mathbf{x}) \quad \mathbf{x} \in \Gamma_{\text{essential}}\,, \tag{3.46}$$

the so-called *natural* boundary conditions are not analogous to the Neumann boundary conditions of the potential theory ($\frac{\partial \mathbf{u}}{\partial \mathbf{n}} = 0$)

$$\mathbf{t}(\mathbf{x}, \mathbf{n}) = \mathbf{g}(\mathbf{x}) \quad \mathbf{x} \in \Gamma_{\text{natural}}\,, \tag{3.47}$$

where $\mathbf{t}(\mathbf{x}, \mathbf{n}) = \boldsymbol{\sigma}(\mathbf{x})\mathbf{n}$ is the Couchy stress vector or the traction, cf. (3.24), and $\mathbf{g}(\mathbf{x})$ is the density of surface forces, which is further assumed vanishing on the free boundary $\mathbf{g}(\mathbf{x}) = 0\,,\ \mathbf{x} \in \Gamma_{\text{natural}}$. With (3.35) the natural boundary conditions (3.47) in the linear elastic approximation can be written in an explicit form respectively the displacement [8]

$$\frac{\nu}{1-2\nu}\,\mathbf{n}\,(\mathrm{div}\,\mathbf{u}) + \frac{\partial \mathbf{u}}{\partial \mathbf{n}} + \frac{1}{2}\,[\,\mathbf{n} \times \mathrm{rot}\,\mathbf{u}\,] = 0\,. \tag{3.48}$$

Special contact problems. Besides the essential and natural boundary conditions described above, special contact problems appear in the modeling of facial tissues. The contact between the different tissue layers, in particular, between the skin and muscle layers, or the sliding phenomena between the lips and the teeth cannot be reduced to the essential or natural boundary conditions. However, the local sliding over the surface $S \subset \Gamma$ can formally be interpreted as a kind of homogeneous essential boundary condition and treated analogously to (3.46) with respect to the projection of the displacement on the the direction of the normal vector

$$\mathbf{u}(\mathbf{x}) \perp \mathbf{n}_S(\mathbf{x}) :\ \mathbf{u}(\mathbf{x})^T\,\mathbf{n}_S(\mathbf{x}) = 0 \quad \mathbf{x} \in S\,, \tag{3.49}$$

where $\mathbf{n}_S(\mathbf{x})$ is the normal vector to the surface S at point $\mathbf{x}$. The handling of linear elastic contact problems is given, for example, in [75].

Boundary value problem. Putting it all together, the boundary value problem (BVP) that describes the deformation of an isotropic and homogeneous hyperelastic material under the impact of external forces in the reference configuration is given by

$$\begin{cases} \mathbf{A}(\mathbf{u}) = \mathbf{f} \quad \text{in } \Omega\,, \\ \mathbf{u}(\mathbf{x}) = \hat{\mathbf{u}}(\mathbf{x}) \quad \mathbf{x} \in \Gamma_{\text{essential}} \subset \Omega\,, \\ \mathbf{t}(\mathbf{x}, \mathbf{n}) = 0 \quad \mathbf{x} \in \Gamma_{\text{natural}} \subset \Omega\,, \end{cases} \tag{3.50}$$

where $\hat{\mathbf{u}}(\mathbf{x})$ is the predefined boundary displacement and

$$\mathbf{A}(\mathbf{u}) = -\text{div}\left\{(\mathbf{I} + \boldsymbol{\nabla}\mathbf{u})\,\boldsymbol{\sigma}(\boldsymbol{\varepsilon}(\mathbf{u}))\right\} \tag{3.51}$$

denotes the operator of non-linear elasticity.

Linear elasticity. Under assumption of small deformations, a completely linear formulation of the BVP (3.50) with respect to the displacement can be derived. The equation of the static equilibrium (3.32) in the linear approximation takes the form

$$-\text{div}\,\boldsymbol{\sigma}(\mathbf{e}(\mathbf{u})) = \mathbf{f}\,, \tag{3.52}$$

where $\mathbf{e}(\mathbf{u})$ is the linearized strain tensor (3.21). The linear elastic approximation can be also interpreted as the first step of the iterative solution scheme (see (3.93))

$$\mathbf{A}'(0)\,\mathbf{u} = \mathbf{f}\,, \tag{3.53}$$

where $\mathbf{A}'(0)$ denotes the first derivative of (3.51). After neglecting all terms of the order higher than 1 with respect to the displacement, (3.53) can be re-written in the following form

$$-\frac{E}{2(1+\nu)}\left(\boldsymbol{\Delta} + \frac{1}{1-2\nu}\,\text{grad}\,\text{div}\right)\mathbf{u}(\mathbf{x}) = \mathbf{f}(\mathbf{x})\,. \tag{3.54}$$

(3.54) yields the explicit relationship between the displacement and the density of applied body forces and is known as the *Lamé-Navier* partial differential equation.

3.3 Finite Element Method

The boundary value problem (3.50) can be generally solved with the help of numerical techniques only. In this work, the finite element method (FEM) is used for modeling and simulation of the deformation of the arbitrary shaped elastic objects. In what follows, the basics of the FEM for solving elliptic partial differential equations and, in particular, the linear and non-linear elastic boundary value problems are described.

Weak formulation. The basic idea of an FE approach is to replace the exact solution $\mathbf{u}(\mathbf{x})$ defined on the function space of the continuous problem $\mathbf{V}$ by an approximative solution $\mathbf{u}_N(\mathbf{x})$ defined on the finite-dimensional subspace $\mathbf{V}_N \subset \mathbf{V}$ as a set of linear independent functions $\varphi_i \in \mathbf{V}_N$ (*basis functions*) building a basis of $\mathbf{V}_N$

$$\mathbf{u}_N(\mathbf{x}) = \sum_{i=1}^{N} \mathbf{u}^i \varphi_i(\mathbf{x}) \,, \tag{3.55}$$

where $\mathbf{u}^i$ are the nodal values for a discrete number of mesh nodes N. Consider

$$\mathbf{L}(\mathbf{u}) = \mathbf{b} \tag{3.56}$$

the linear elliptic PDE to be solved. The approximative solution (3.55) in (3.56) produces the *residual error* or *residuum* such that

$$\mathbf{L}(\mathbf{u}_N) - \mathbf{b} = \mathbf{r} \neq 0 \,. \tag{3.57}$$

Since it is usually impossible to force the residuum $\mathbf{r}$ to be zero for each node, the error can be distributed in the domain Ω with *weighting functions* ψ_j

$$\sum_{j=1}^{N} \int_{\Omega} \mathbf{r}\, \psi_j \, dV = 0 \,. \tag{3.58}$$

The technique of solving PDEs based on (3.58) is called the *method of weighted residuals*. Furthermore, if the function subspace that spans the basis $\{\psi_1, \psi_2, ...\psi_N\}$ is identical with the subspace $\mathbf{V}_N$, i.e., the weighting functions are identical with the basis functions, (3.58) defines the projection of the exact solution $\mathbf{u}$ of the problem (3.56) over the space $\mathbf{V}_N$

$$\langle \mathbf{r},\, \varphi_j \rangle = 0 \,,\ \forall j \tag{3.59}$$

where $\langle \cdot\,,\, \cdot \rangle$ notifies the L_2 scalar product in the *Sobolev space* $H^1(\Omega)$. The formulation of the FEM based on (3.59) is known as the *Galerkin* method.

The method of weighted residuals applied to continuum mechanics problems can be also interpreted as a variational problem of energy minimization. Consider the equation of the static equilibrium in the linear approximation (3.52). The weighted residuum (3.58) formulated with $\mathbf{r} = \operatorname{div}\boldsymbol{\sigma} + \mathbf{f}$ and test displacements $\boldsymbol{v} : \Omega \to \mathbb{R}^3$ as weighting functions

$$\langle(\operatorname{div}\boldsymbol{\sigma} + \mathbf{f}),\, \boldsymbol{v}\rangle \;=\; \langle\operatorname{div}\boldsymbol{\sigma},\, \boldsymbol{v}\rangle \;+ \langle\mathbf{f},\, \boldsymbol{v}\rangle \;= 0 \tag{3.60}$$

is identical to the *principle of virtual work* that postulates "the balance of work of all forces along the *virtual displacement*". Applying the fundamental *Green's formula* [42] to the first term in (3.60)

$$\langle\operatorname{div}\boldsymbol{\sigma},\, \boldsymbol{v}\rangle \;= -\langle\boldsymbol{\sigma},\, \boldsymbol{\nabla}\boldsymbol{v}\rangle \;+ \int\limits_{\partial\Omega} \boldsymbol{\sigma}\mathbf{n}\, dS\,. \tag{3.61}$$

and recalling that $\boldsymbol{\nabla}\boldsymbol{v} = \mathbf{e}(\boldsymbol{v})$ and $\boldsymbol{\sigma}\mathbf{n} = 0$ we then write (3.60)

$$\langle\boldsymbol{\sigma}(\mathbf{e}(\mathbf{u})),\, \mathbf{e}(\boldsymbol{v})\rangle \;= \langle\mathbf{f},\, \boldsymbol{v}\rangle\,, \tag{3.62}$$

or under consideration of the strain-stress relationship $\boldsymbol{\sigma}(\mathbf{e}(\mathbf{u})) = \mathbf{C}\,\mathbf{e}(\mathbf{u})$

$$\langle\mathbf{C}\,\mathbf{e}(\mathbf{u}),\, \mathbf{e}(\boldsymbol{v})\rangle \;= \langle\mathbf{f},\, \boldsymbol{v}\rangle\,. \tag{3.63}$$

Summarizing, we make a conclusion that finding an approximate solution of the BVP (3.50) (*strong formulation*) in the discrete functional subspace $\mathbf{V}_N$ is formally equivalent to finding a solution of the corresponding *weak formulation*

$$a(\mathbf{u},\, \boldsymbol{v}) = l(\boldsymbol{v})\;\forall\boldsymbol{v} \in \mathbf{V}_N\,, \tag{3.64}$$

where

$$\begin{aligned} a(\mathbf{u},\, \boldsymbol{v}) &= \langle\mathbf{C}\,\mathbf{e}(\mathbf{u}),\, \mathbf{e}(\boldsymbol{v})\rangle\,,\\ l(\boldsymbol{v}) &= \langle\mathbf{f},\, \boldsymbol{v}\rangle\,. \end{aligned} \tag{3.65}$$

Since (3.65) results from the linear elastic approximation of (3.50), the derivation of the weak form of the non-linear elastic BVP is analogous.

Existence and uniqueness of the weak solution. Now, we provide a brief outline of the existence and the uniqueness of the weak formulation (3.64) of the linearized BVP (3.50) as it is stated in [21]. For a detailed review of the variational formulation of elliptic PDEs as well as the existence theory, we refer to the corresponding literature, for example [20, 11].

Following theorem gives the definition of the $\mathbf{V}$-ellipticity of a bilinear form $a(\cdot\,,\cdot)$ and that the *quadratic functional* $J(\boldsymbol{v}) = \frac{1}{2}a(\mathbf{u},\, \boldsymbol{v}) - l(\boldsymbol{v})$ related to the weak formulation (3.64) has an unique solution.

Theorem 1 *Let* $\mathbf{V}$ *be a Banach space with norm* $\|\cdot\|$*, let* $l : \mathbf{V} \to \mathbb{R}$ *be a continuous linear form, and let* $a(\cdot\,,\cdot) : \mathbf{V} \times \mathbf{V} \to \mathbb{R}$ *be a symmetric continuous* $\mathbf{V}$*-elliptic bilinear form in the sense that there exists a constant* β *such that*

$$\beta > 0 \text{ and } a(\boldsymbol{v}, \boldsymbol{v}) \geq \beta \|\boldsymbol{v}\|^2, \quad \forall \boldsymbol{v} \in \mathbf{V}.$$

Then the problem: Find $\mathbf{u} \in \mathbf{V}$ *such that*

$$a(\mathbf{u}, \boldsymbol{v}) = l(\boldsymbol{v}) \quad \forall \boldsymbol{v} \in \mathbf{V},$$

has one and only one solution, which is also the unique solution of the problem: Find $\mathbf{u} \in \mathbf{V}$ *such that*

$$J(\mathbf{u}) = \inf_{v \in V} J(\mathbf{u}), \text{ where } J : \boldsymbol{v} \in \mathbf{V} \to J(\mathbf{u}) = \frac{1}{2} a(\mathbf{u},\, \boldsymbol{v}) - l(\boldsymbol{v})$$

■

The generalization of the theorem 1 for the case of the non-symmetric bilinear form is stated by the *Lax-Milgram lemma* [20].

Remark. The functional J is *convex* in the sense that

$$J''(\boldsymbol{v}) \geq 0 \quad \forall \boldsymbol{v} \in \mathbf{V}$$

and it satisfi es a*coerciveness inequality*:

$$J(\mathbf{u}) = \frac{1}{2} a(\mathbf{u},\, \boldsymbol{v}) - l(\boldsymbol{v}) \geq \frac{\beta}{2} \|\boldsymbol{v}\|^2 - \|l\|\, \|\boldsymbol{v}\| \quad \forall \boldsymbol{v} \in \mathbf{V}\,.$$

In order to decide in which particular space $\mathbf{V}$ one should seek a solution of the weak formulation (3.64), we observe that

$$a(\mathbf{u},\, \boldsymbol{v}) = \langle \mathbf{C}\, \mathbf{e}(\mathbf{u}),\, \mathbf{e}(\boldsymbol{v}) \rangle \;=$$
$$\lambda \langle\, \mathrm{tr}\, \mathbf{e}(\mathbf{u}),\; \mathrm{tr}\, \mathbf{e}(\boldsymbol{v}) \rangle + 2\mu \langle \mathbf{e}(\mathbf{u}),\, \mathbf{e}(\boldsymbol{v}) \rangle \;\geq\; 2\mu \langle \mathbf{e}(\mathbf{u}),\, \mathbf{e}(\boldsymbol{v}) \rangle\,,$$

which follows from (3.36). Hence the $\mathbf{V}$-ellipticity of $a(\cdot\,,\cdot)$ will follow if it can be shown that, *on the space* $\mathbf{V}$*, the semi-norm*

$$\boldsymbol{v} \in H^1(\Omega) \to |\mathbf{e}(\boldsymbol{v})|_{0,\Omega} = \{ \langle \mathbf{e}(\mathbf{u}),\, \mathbf{e}(\boldsymbol{v}) \rangle \}^{\frac{1}{2}}$$

is a norm, equivalent to the norm $\|\cdot\|_{1,\Omega}$*.* This results from the following fundamental *Korn's inequality*.

Theorem 2 *Let Ω be a domain in $\mathbb{R}^3$. For each $\boldsymbol{v} = (v_i) \in H^1(\Omega)$, let*

$$\mathbf{e}(\boldsymbol{v}) = (\frac{1}{2}(\partial_j v_i + \partial_i v_j)) \in \mathbf{L}^2(\Omega)\,.$$

Then there exists a constant $c > 0$ such that

$$\|\boldsymbol{v}\|_{1,\Omega} \leq c\{|\boldsymbol{v}|^2_{0,\Omega} + |\mathbf{e}(\boldsymbol{v})^2_{0,\Omega}|\}^{\frac{1}{2}} \quad \forall \boldsymbol{v} \in H^1(\Omega)\,,$$

and thus, on the space $H^1(\Omega)$, the mapping

$$\boldsymbol{v} \rightarrow \{|\boldsymbol{v}|^2_{0,\Omega} + |\mathbf{e}(\boldsymbol{v})|^2_{0,\Omega}\}^{\frac{1}{2}}$$

is a norm, equivalent to the norm $\|\cdot\|_{1,\Omega}$. ■

With Korn's inequality, it can be further shown that

$$c^{-1}\|\boldsymbol{v}\| \leq |\mathbf{e}(\boldsymbol{v})|^2_{0,\Omega} \leq c^1\|\boldsymbol{v}\| \quad \forall \boldsymbol{v} \in \mathbf{V}$$

(see Theorem 6.3-4., [21]) and that the bilinear form $\boldsymbol{v} \rightarrow \langle \mathbf{e}(\mathbf{u}),\, \mathbf{e}(\boldsymbol{v})\rangle$ and consequently the bilinear form $a(\mathbf{u},\, \boldsymbol{v})$ are $\mathbf{V}$-elliptic.

Assembling the previous results, the existence of a solution $\mathbf{u} \in H^1(\Omega)$ of the weak form of the linear elastic BVP (3.64), the so-called *weak solution* can be established, see Theorem 6.3-5. [21].

The proof of the existence and the uniqueness of the weak form of the nonlinear elastic BVP in conjunction with the discussion of different iterative solution schemes is in given [20, 21].

Abstract error estimate. With each functional subspace $\mathbf{V}_N \subset \mathbf{V}$ is associated the discrete solution $\mathbf{u}_N$ that satisfies

$$a(\mathbf{u}_N,\, \boldsymbol{v}_N) = l(\boldsymbol{v}_N) \quad \forall \boldsymbol{v}_N \in \mathbf{V}_N \tag{3.66}$$

and should be *convergent* in the sense that

$$\lim_{N\rightarrow\infty} \|\mathbf{u} - \mathbf{u}_N\| = 0\,. \tag{3.67}$$

We are interested in giving sufficient conditions for convergence and the abstract error estimate. This can be done by using the following theorem [11]

Theorem 3 *(Cea's lemma). Let $a(\cdot,\,\cdot)$ be a bilinear $\mathbf{V}$-elliptic form and $\mathbf{u}$ and $\mathbf{u}_N$ are the exact and discrete solution of the variational problem over $\mathbf{V}$ and $\mathbf{V}_N \subset \mathbf{V}$ respectively. There exists a constant C independent of the subspace $\mathbf{V}_N$ such that*

$$\|\mathbf{u} - \mathbf{u}_N\| \leq C \inf_{\boldsymbol{v}_N \in V_N} \|\mathbf{u} - \boldsymbol{v}_N\|$$

■

$C = 1$ for elliptic PDE. Cea's lemma has several important consequences for the choice of the proper solution subspace and the whole discretization scheme.

Locking effect. In finite element computations of solid mechanics problems, it is sometimes observed that the discrete solution of the given BVP significantly diverges from the theoretically predicted one. A collective term for such deviations is called by engineers the *locking effect*, since the obtained numerical solution often yields too small displacements in comparison with the theory. The locking effect may happen due to several reasons. From the mathematical point of view, the problem consists in the dependence of the constant C in Cea's lemma (theorem 3) on a small parameter α, which causes strong increase of C by approaching to some critical value $\alpha \to \alpha_C$. In [11], some particular cases of the locking effect are described.

Poisson-locking. This type of the locking effect results from the strong dependence of $C(\nu)$ on the Poisson ratio ν in the case of the bilinear form (3.64)

$$a(\mathbf{u},\,\boldsymbol{v}) = \int_\Omega \frac{E}{1+\nu}\left(\frac{\nu}{1-2\nu}\langle\,\mathrm{tr}\,\mathbf{e}(\mathbf{u}),\,\mathrm{tr}\,\mathbf{e}(\boldsymbol{v})\rangle + \langle\mathbf{e}(\mathbf{u}),\mathbf{e}(\boldsymbol{v})\rangle\right) dV \quad (3.68)$$

with a singularity occurring by $C(\nu = 0.5) = \infty$. To avoid the Poisson locking of the *pure displacement formulation* (3.68) for the incompressible material with $\nu = 0.5$, the so-called *mixed formulation* of (3.64) with an additional variable, pressure $p : \Omega \to \mathbb{R}$ resulting in a (non-elliptic) *saddle point problem* is proposed

$$\begin{aligned} &\langle p,\,\mathrm{tr}\,\mathbf{e}(\boldsymbol{v})\rangle + \frac{E}{1+\nu}\langle\mathbf{e}(\mathbf{u}),\mathbf{e}(\boldsymbol{v})\rangle = l(\boldsymbol{v}) \quad \boldsymbol{v} \in H^1(\Omega), \quad p \in L_2(\Omega) \\ &\langle q,\,\mathrm{tr}\,\mathbf{e}(\mathbf{u})\rangle = 0 \quad q \in L_2(\Omega) \end{aligned} \quad (3.69)$$

Besides the Poisson-locking there are several other types of the locking effect, which for instance may result from the insufficient order of the interpolating functions as it is observed for shells and membranes. Thus, the occurrence of the

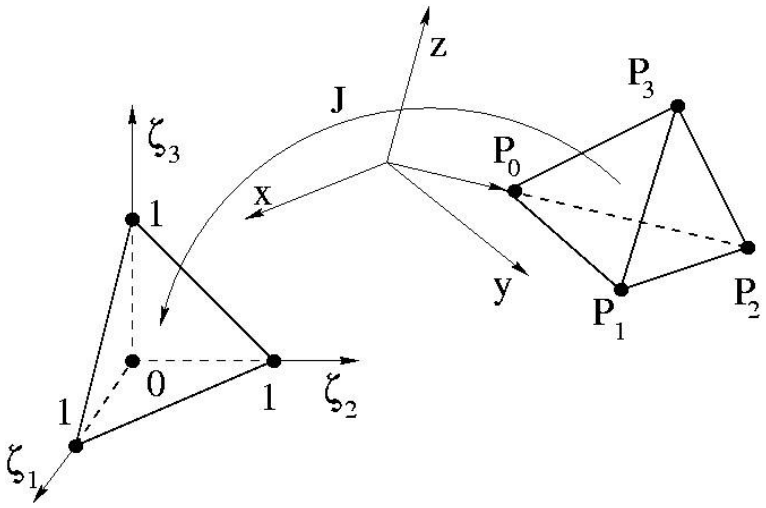

Figure 3.8: Arbitrary and reference tetrahedron.

locking effect should be taken into account and investigated in each particular case. Finally, it is to be mentioned that one of the general measures proposed to avoid the locking is the so-called *reduced integration* [56, 11], which consists in taking a preferably low number of sample points for the numerical integration via Gauss-Legendre quadrature.

Finite elements. The basic idea of the finite element discretization method consists in finding an approximate solution of the continuous problem for a discrete number of mesh nodes. For this purpose, the domain Ω occupied by a physical body has to be subdivided into a discrete number of not overlapping subdomains Ω_i, the so-called *finite elements*, such that $\Omega = \bigcup \Omega_i$ and $\Omega_i \cap \Omega_j = \emptyset,\ i \neq j$. In this work, domain partitioning based on the tetrahedral 3D elements is used. Allowing flexible triangulation of arbitrary 3D domains, tetrahedral elements are widely used in the finite element analysis of solid structures [109]. In Figure 3.8, the arbitrary and reference tetrahedron are shown. Consequently, all continuous variables of the problem have to be interpolated with basis functions in accordance with (3.55). From the numerical point of view it is more advantageous, if the resulting system of equations associated with the discrete problem has a sparse structure. This is the case if the basis functions φ_i have *local supports*, i.e.,

$$\varphi_i(\mathbf{x}_j) = \delta_{ij}\ ,\ i,j = 1...N\ . \tag{3.70}$$

Furthermore, the basis functions have to satisfy other additional constraints such as the requirements to have a predefined behavior and to be continuous on each

subdomain Ω_i, as well as to be of the order that is sufficient for the approximation of the highest order derivatives in the weak form of the corresponding BVP. In the weak form of both linear and non-linear elastic BVPs, only the first order derivatives have to be approximated. Hence, the simplest interpolation of elastic continuum with linear basis functions is possible. Linear basis functions satisfying the above requirements and corresponding to the reference tetrahedron in Figure 3.8 are

$$\begin{aligned} \varphi_1 &= 1 - \xi_1 - \xi_2 - \xi_3, \\ \varphi_2 &= \xi_1, \\ \varphi_3 &= \xi_2, \\ \varphi_4 &= \xi_3. \end{aligned} \tag{3.71}$$

Besides the linear basis functions, quadratic, cubic and higher order polynomials can be used as admissible basis functions. On the one hand, the non-linear basis functions enable more smooth interpolation. On the other hand, higher order polynomial require additional nodes to be placed in the middle of the edges and faces of the tetrahedron. Since the quadratic interpolation requires $N = 10$ and the cubic interpolation already $N = 20$ nodes per element, the dimension of the system matrix $O(3N \times 3N)$ increases for non-linear elements dramatically. Furthermore, the precision of the numerical solution cannot be substantially improved with the increasing smoothness of the interpolating functions, but with the sufficient domain refinement ([11], see comments to Cea's lemma).

Since the basis functions (3.71) are defined on the reference tetrahedron with the unit edge length $\xi_i \in [0, 1]$, each arbitrary tetrahedron with node coordinates x_i^n has to be mapped onto the reference one, see Figure 3.8. Such mapping is described by the general *Jacobi transformation*

$$\mathbf{x} = \mathbf{J}\,\boldsymbol{\xi}\,, \tag{3.72}$$

where **J** is the corresponding Jacobi matrix

$$\mathbf{J} = \frac{\partial x_i}{\partial \xi_j} = \begin{pmatrix} (x_1^2 - x_1^1) & (x_1^3 - x_1^1) & (x_1^4 - x_1^1) \\ (x_2^2 - x_2^1) & (x_2^3 - x_2^1) & (x_2^4 - x_2^1) \\ (x_3^2 - x_3^1) & (x_3^3 - x_3^1) & (x_3^4 - x_3^1) \end{pmatrix}. \tag{3.73}$$

The inverse transformation is then

$$\boldsymbol{\xi} = \mathbf{J}^{-1}\,\mathbf{x} = \frac{\mathbf{J}^T}{6V_t}\,\mathbf{x}\,, \tag{3.74}$$

where $\mathrm{V}_t = |\mathbf{J}|/6$ is the volume of a tetrahedron (x_i^n), and thus the condition of the inverse Jacobi matrix decisively depends on the geometry of the tetrahedral element.

Linear elastic FEM. The starting point for the linear elastic FEM is the weak formulation (3.64) of the linearized BVP (3.50). Comprising the previous results, we seek for the discrete solution $\mathbf{u}_N \in \mathbf{V}_N \subset \mathbf{V}$ of the following BVP

$$\begin{cases} \int\limits_{\Omega} \mathbf{C}\mathbf{e}(\mathbf{u}_N)\, \mathbf{e}(\boldsymbol{v}_N)\, dV = \int\limits_{\Omega} \mathbf{f}\, \boldsymbol{v}_N\, dV \quad \text{in } \Omega\,, \\ \mathbf{e}(\mathbf{u}_N) = \dfrac{1}{2}(\boldsymbol{\nabla}\mathbf{u}_N^T + \boldsymbol{\nabla}\mathbf{u}_N)\,, \\ \mathbf{u}_N = \sum\limits_{i=1}^{N} \mathbf{u}^i \varphi_i\,,\ \boldsymbol{v}_N = \sum\limits_{i=1}^{N} \boldsymbol{v}^i \varphi_i\,, \\ \mathbf{u}_N(\mathbf{x}) = \hat{\mathbf{u}}_N(\mathbf{x}) \quad \mathbf{x} \in \Gamma \subset \Omega\,, \end{cases} \tag{3.75}$$

or componentwise in a more explicit form

$$u_k^p \int\limits_{\Omega} C_{ijkm}\, \partial_k \varphi_p\, \partial_j \varphi_q\, dV = \int\limits_{\Omega} f_i \varphi_q\, dV\,, \tag{3.76}$$

where $i, j, k, m = 1, 2, 3$, $p, q = 1...N$, $\{u_j^i\}$ denotes the $3 \times N$ vector of nodal values and

$$C_{ijkm} = \lambda\, \delta_{ij}\delta_{km} + \mu\, (\delta_{ik}\delta_{jm} + \delta_{im}\delta_{jk})\,. \tag{3.77}$$

The partial derivatives of the basis functions $\varphi(\boldsymbol{\xi})$ in (3.76) have to be calculated as follows

$$\frac{\partial \varphi_k}{\partial x_j} = \frac{\partial \varphi_k}{\partial \xi_i}\frac{\partial \xi_i}{\partial x_j} = \frac{\partial \varphi_k}{\partial \xi_i}\, \mathbf{J}^{-1}\,. \tag{3.78}$$

Here, it is one more time to be pointed out that because of $\mathbf{J}^{-1} \sim \frac{1}{V_t}$ the gradient fi eld (3.78) and consequently $\boldsymbol{\nabla}\mathbf{u}$ depends on the quality of the discretization. In particular, degenerated tetrahedrons with $V_t \approx 0$ can cause the deterioration of the resulting system condition.

Further, the volume integrals on both sides of (3.78) are usually to be computed numerically via Gauss-Legendre quadrature. Recalling the discussion about the locking effect, integration with one Gauss point is used in this work, which also shortens the assembly time.

The system (3.76) can be written in a matrix form

$$\mathbf{A}\,\mathbf{u} = \mathbf{b}, \tag{3.79}$$

where $\mathbf{u}$ is the vector of nodal values, the right-hand side vector $\mathbf{b}$ is known as *load vector* and the $3N \times 3N$ matrix $\mathbf{A}$ is called the *stiffness matrix*. The stiffness

matrix basically contains the integrals over all volume elements of the domain of interest, which are stored in N^2-th 3×3 nodal stiffness matrices $\mathbf{A}_{ij}^{nm}$, where $n, m = 0...(N-1)$ are nodal indexes and $i, j = 0, 1, 2$.

As a consequence of the local support of basis functions and a finite number of node neighbors for each mesh node the stiffness matrix consists of a small number of non-zero elements. Thereby, the structure of i-th row of the stiffness matrix reflects the structure of i-th node neighborhood in a mesh: the maximum number of non-zero elements of i-th row is equal to $3 \times N_i$, where N_i is the number of i-th node neighbors. Such a sparse structure enables a very compact storage of the stiffness matrix, and is also of crucial importance for the application of the efficient solving algorithms.

Since the bilinear form $a(\cdot\,,\,\cdot)$ is symmetric and $\mathbf{V}$-elliptic, the resulting stiffness matrix $\mathbf{A}$ is symmetric and positive definite as well. These properties are important for the application of the efficient numerical techniques for the solution of (3.79).

Incorporation of boundary conditions. In order to obtain a non-trivial solution, the linear system of equations (3.79) has to be modified with respect to the given boundary conditions. Generally, the boundary conditions are given in the form of

- prescribed boundary displacements, which is usually the case in soft tissue modeling and medical imaging analysis, and/or
- applied forces.

In the first case, the solution has to be obtained from the modified system

$$\hat{\mathbf{A}}\mathbf{u} = \hat{\mathbf{b}}, \tag{3.80}$$

where $\hat{\mathbf{A}}$ is the stiffness matrix with incorporated prescribed displacements $\hat{\mathbf{u}}$ and $\hat{\mathbf{b}} = -\mathbf{A}\hat{\mathbf{u}}$ is the load vector corresponding to the prescribed boundary displacements $\hat{\mathbf{u}}$. The incorporation of the prescribed displacement of i-th node, i.e., the essential boundary condition, consists in setting i-th row and i-th column of $\mathbf{A}$ to zero and setting the i-th diagonal element of $\mathbf{A}$ to identity $A_{ii} = 1$. The homogeneous natural boundary conditions $\mathbf{t} = \boldsymbol{\sigma}\mathbf{n} = 0$, cf. (3.50), require in the finite element method no extra implementation, since they are implicitly considered by the assembly of the stiffness matrix. The transformed stiffness matrix $\hat{\mathbf{A}}$ still has to be symmetric and positive definite, in order the modified system (3.80) to have a non-trivial and unique solution.

Iterative numerical techniques. In order to solve linear and non-linear systems of equations, iterative numerical techniques are usually applied. Hence, we briefly describe the method of conjugate gradients and the Newton method, which have been used in this work for iterative solving linear and non-linear elliptic problems, respectively.

Method of conjugate gradients. The linear elastic finite element method leads to the linear system of equations $\mathbf{A}\mathbf{u} = \mathbf{b}$ respectively the nodal displacements $\mathbf{u}$ with the symmetric, positive definite and sparsely occupied stiffness matrix $\mathbf{A}$. This properties enable the application of the efficient solving technique, the *method of conjugate gradients* (CG) [57].

The common idea of the iterative methods is to approach the solution of the given problem $\mathbf{u}$ by the successive approximations $\mathbf{u}^k$ starting from some initial guess $\mathbf{u}^0$. The approximate solution is searched to minimize the residual difference $\|\mathbf{u} - \mathbf{u}^k\|$ w.r.t. an abstract norm $\|\cdot\|$. A general approach to the formulation of the CG method is based on the *Ritz-Galerkin approximation* of the solution in the *Krylov spaces* with the scalar product

$$(\mathbf{x},\, \mathbf{y}) = \mathbf{x}^T \mathbf{A} \mathbf{y} \tag{3.81}$$

and the corresponding norm, the so-called energy norm,

$$\|\mathbf{y}\|_A = \sqrt{(\mathbf{y},\, \mathbf{y})} \tag{3.82}$$

defined for each symmetric, positive definite matrix$\mathbf{A}$. Consequently, the main operation of the CG algorithm is the matrix-vector multiplication, which in the case of a sparsely occupied matrix can be performed particularly efficient. For a detailed derivation of the CG method, we refer to [30].

The CG algorithm requires no additional parameters to achieve the given precision of the solution ϵ

$$\epsilon = \frac{\|\mathbf{u} - \mathbf{u}^k\|_A}{\|\mathbf{u} - \mathbf{u}^0\|_A} \tag{3.83}$$

after maximum n iterations

$$n \sim \frac{1}{2}\sqrt{\kappa} \ln\left(\frac{2}{\epsilon}\right) + 1\,. \tag{3.84}$$

κ in (3.84) denotes the *condition number* of the system matrix $\mathbf{A}$ with maximal and minimal eigenvalues $\lambda_{\max}$ and $\lambda_{\min}$, respectively

$$\kappa = \frac{\lambda_{\max}}{\lambda_{\min}}\,. \tag{3.85}$$

Preconditioning. As we have seen above, the convergence of the CG algorithm essentially depends on the condition of the system determined by the condition number κ (3.85). For ill-conditioned and, in particular, quasi-singular systems, i.e. the minimal eigenvalue is close to zero $0 < \lambda_{min} \ll 1$, the condition number is large $\kappa \gg 1$ and the convergence rate of the CG method becomes worse. In this case, the performance of the iteration process can be improved by decreasing the condition number with the help of preconditioning algorithms.

The idea of preconditioning is to replace the original, ill-conditioned system $\mathbf{A}\mathbf{u} = \mathbf{b}$ with the modified one, which has a better condition number close to 1. There are several well established strategies for the acceleration of the convergence process in the finite element calculations, see for example [109]. The choice of the preconditioning method depends on the symmetry, the condition, the dimension and other characteristics of the concrete problem, since the preconditioning algorithms substantially differ in the performance and the complexity. In this work, the comparatively simple and fast *Jacobi preconditioning* is used. This method consists in scaling the original system

$$\hat{A}_{ij} = D_i \, A_{ij} \, D_j \,, \tag{3.86}$$

where

$$D_i = 1/\sqrt{A_{ii}} \,. \tag{3.87}$$

Such scaling yields the symmetric and positive definite matrix $\mathbf{A}$ is transformed into the symmetric and positive definite matrix $\hat{\mathbf{A}}$ of the following structure

$$\hat{\mathbf{A}} = \begin{cases} \hat{A}_{ij} = 1, \; i = j \\ \hat{A}_{ij} < 1, \; i \neq j \end{cases} \tag{3.88}$$

For the range of problems studied in this work, such scaling already yields a sufficient improvement of the performance. However, in the case of the large and ill-conditioned system the application of more sophisticated preconditioning techniques such as multigrid methods should be taken into consideration [11].

Iterative solution of non-linear problems. The major difficulty in the numerical computation of deformations of elastic structures is the proper handling of various non-linearities occurring in the boundary value problem (3.50). A general approach for solving non-linear problems consists in a successive approximation of the solution by a set of corresponding linearized problems. Assuming that the boundary value problem (3.50) has an approximate solution $\mathbf{u}^n$

$$\mathbf{A}(\mathbf{u}^n) = \mathbf{f}^n \,, \tag{3.89}$$

we firstly define the next $(n+1)$-st approximate displacement

$$\mathbf{u}^{n+1} = \mathbf{u}^n + \delta\mathbf{u}^n\,, \tag{3.90}$$

where $\delta\mathbf{u}^n = \mathbf{u}^{n+1} - \mathbf{u}^n$ denotes the $(n+1)$-st displacement increment. Applying the *Taylor formula* to (3.51) at the point $\mathbf{u}^{n+1}$ one obtains

$$\mathbf{A}(\mathbf{u}^{n+1}) = \mathbf{A}(\mathbf{u}^n + \delta\mathbf{u}^n) = \mathbf{A}(\mathbf{u}^n) + \mathbf{A}'(\mathbf{u}^n)\delta\mathbf{u}^n + o(\delta\mathbf{u}^n)\,, \tag{3.91}$$

where $\mathbf{A}'(\mathbf{u}^n)$ is the *Fréchet derivative*, also known as the *tangent stiffness*. Recalling that

$$\mathbf{A}(\mathbf{u}^{n+1}) - \mathbf{A}(\mathbf{u}^n) = \mathbf{f}^{n+1} - \mathbf{f}^n = \delta\mathbf{f}^n\,, \tag{3.92}$$

where $\delta\mathbf{f}^n$ denotes an increment of body forces corresponding to $\delta\mathbf{u}^n$, (3.91) can be re-written as follows

$$\mathbf{A}'(\mathbf{u}^n)\delta\mathbf{u}^n = \delta\mathbf{f}^n\,. \tag{3.93}$$

Thus, the application of the iterative solution scheme results in a successive approximation of the $(n+1)$-st displacement by solving a set of linear equations (3.93) respectively to the displacement increment with a subsequently update (3.90). In what follows, we briefly discuss well established iterative techniques for solving non-linear problems of structural mechanics.

Method of incremental loads. The basic idea of the incremental method is to let the body forces vary by a small force increment

$$\delta\mathbf{f}^n = (\lambda^{n+1} - \lambda^n)\mathbf{f},\ 0 \le \lambda^n \le 1\,, \tag{3.94}$$

from 0 to the given force $\mathbf{f}$, and to compute successive approximations $\mathbf{u}^{n+1}$ to the exact solution $\mathbf{u}(\lambda^{n+1}\mathbf{f})$ by solving a set of linear equations

$$\begin{aligned} &\mathbf{A}'(\mathbf{u}^n)\delta\mathbf{u}^n = (\lambda^{n+1} - \lambda^n)\mathbf{f} \\ &\mathbf{u}^{n+1} = \mathbf{u}^n + \delta\mathbf{u}^n \end{aligned} \tag{3.95}$$

The detailed description of the incremental method, including the proof of the existence and the uniqueness of the solution of the non-linear elastic BVP based on it, can be found in [21].

Newton method. The Newton method for solving a non-linear problem of the type $\mathbf{A}(\mathbf{u}) = \mathbf{f}$ consists in successively solving a set of linearized equations

$$\mathbf{A}'(\mathbf{u}^n)(\mathbf{u}^{n+1} - \mathbf{u}^n) = \mathbf{f} - \mathbf{A}(\mathbf{u}^n)\,,\ n \geq 0 \tag{3.96}$$

starting with an initial guess $\mathbf{u}^0$.

In accordance with (3.96), each iteration step the tangent stiffness matrix has to be assembled anew. Since such full update of $\mathbf{A}'(\mathbf{u}^n)$ at each iteration step is relatively time consuming, the *simplified* Newton method consisting in using only the first Fréchet derivative $\mathbf{A}'(\mathbf{u}^0)$ can be applied

$$\mathbf{A}'(\mathbf{u}^0)(\mathbf{u}^{n+1} - \mathbf{u}^n) = \mathbf{f} - \mathbf{A}(\mathbf{u}^n)\,,\ n \geq 0\,. \tag{3.97}$$

In this case, the most expensive part of the non-linear calculation, the assembly of the tangent stiffness matrix has to be performed only once. An extensive description of the Newton method in structural mechanics can be found in [24]. Various aspects of application of the Newton method to the "almost singular" problems, which often arise in continuum mechanics, are in [29]. A promising approach for efficient solving non-linear elliptic problems with the help of the *inexact* Newton method is proposed in [32, 33].

Non-linear elastic FEM. A more general approach is based on the weak formulation of the original non-linear elastic boundary value problem (3.50). As we have seen above, the solution of the non-linear elastic BVP can be reduced to the iterative process consisting in recursively solving the system of equations linearized respectively the displacement increment $\boldsymbol{\delta}\mathbf{u}$. For the rest, the finite element discretization of the non-linear elastic BVP is analogous to the linear elastic one. All relevant variables have to be represented in the finite element space $\mathbf{V}_N$ as weighted sums (3.55) and set into (3.93). The linearization of (3.93) simply consists in deleting all the terms that are non-linear with respect to the displacement increment $\boldsymbol{\delta}\mathbf{u}^n$. The weak form of (3.93) can be written componentwise as follows, cf. (3.76)

$$\delta u_k^{p,n} \int\limits_\Omega C'_{ijkm}(\boldsymbol{\nabla}\mathbf{u}^n)\,\partial_k\varphi_p\,\partial_j\varphi_q\,dV = \int\limits_\Omega \delta f_i^n \varphi_q\,dV\,, \tag{3.98}$$

where $i, j, k, m = 1, 2, 3$, $p, q = 1...N$, $n \geq 0$ is the iteration index and

$$C'_{ijpq}(\boldsymbol{\nabla}\mathbf{u}^n) = C_{ijpq} + C_{kjpq}\partial_k u_i^n + C_{ijrp}\partial_r u_q^n + C_{kjpr}\partial_r u_q^n \partial_k u_i^n + C_{pjsr}\varepsilon_{sr}(\mathbf{u}^n)\delta_{iq} \tag{3.99}$$

denotes the tangent stiffness. With $\delta f_i^n = (\lambda^{n+1} - \lambda^n) f_i = h^n f_i$ (3.98) already represents the discrete form of the incremental method (3.95)

$$\delta u_k^{p,n} \int_\Omega C'_{ijkm}(\boldsymbol{\nabla} \mathbf{u}^n)\, \partial_k \varphi_p\, \partial_j \varphi_q\, dV = \int_\Omega h^n f_i \varphi_q\, dV\,. \tag{3.100}$$

The major drawback of the incremental method is that its convergence depends on the step width h^n, which usually should be chosen "small enough" in order to stay "close to path". As a result of this, comparatively large number of iterations of the incremental method is required. Moreover, the incremental method is usually used in finite element analysis of solid structures as a "predictor", which firstly provides the starting solution for an iterative "corrector" [24], for example Newton method. Such coupled incremental/iterative solution scheme is relatively expensive. Instead of this, we use the linear elastic approximation as a one-step predictor and the Newton method as a corrector.

The weak form of the Newton method is given by

$$\delta u_k^{p,n} \int_\Omega C'_{ijkm}(\boldsymbol{\nabla} \mathbf{u}^n)\, \partial_k \varphi_p\, \partial_j \varphi_q\, dV = \int_\Omega f_i \varphi_q\, dV - \mathbf{A}(\mathbf{u}^n)\,, \tag{3.101}$$

with

$$\mathbf{A}(\mathbf{u}^n) = \int_\Omega (\delta_{kl} + u_k^{p,n} \partial_l \varphi_p) \sigma_{lj}(\mathbf{u}^n)\, \partial_j \varphi_q\, dV\,. \tag{3.102}$$

This integral has to be computed without any linearization so that the stress tensor $\sigma_{ij} = C_{ijkm}\, \varepsilon_{km}$ in (3.102) is now associated with the fully non-linear strain tensor $\varepsilon_{ij} = \frac{1}{2}(\partial_j u_i + \partial_i u_j + \partial_i u_l \partial_j u_l)$.

The solution of (3.101) yields the n-th increment of the displacement vector $\delta u_i^n = u_i^{n+1} - u_i^n$. Thus, the application of the iterative solution scheme results in a successive approximation of the $(n+1)$-st displacement

$$\mathbf{u}^{n+1} = \mathbf{u}^n + \delta \mathbf{u}^n. \tag{3.103}$$

For each iteration, the linear system of equations (3.96) respectively the n-th increment of the displacement vector is solved by using the preconditioned conjugate gradients method (PCG).

For the monitoring of the convergence process of the Newton method, a criterion based on the norm of the residual vector $\|\mathbf{r}^n\| = \|\mathbf{f} - \mathbf{A}(\mathbf{u}^n)\|$ is applied. The same criterion is also used for termination of the iterative process

$$\frac{\|\mathbf{r}^n\|}{\|\mathbf{r}^0\|} \leq 10^{-3}\,. \tag{3.104}$$

The straightforward computation of the tangent stiffness (3.99), i.e. the full update of the tangent stiffness matrix at each iteration step, is time consuming. As it has already been mentioned above, this can be substituted with a weaker formulation, the simplified Newton method, where the first Fréchet derivative $\mathbf{A}'(\mathbf{u}^0)$ has to be computed only once.

An additional improvement of performance can be achieved by applying the true non-linear assembly of elementary stiffness matrix $C'_{ijkm}(\boldsymbol{\nabla}\mathbf{u}^n)$ on large deformed elements only. Indeed, if higher order terms in (3.99) are small in comparison with the first linear one C_{ijkm}, they simply can be neglected as it is assumed in linear elasticity. Such mixed linear/non-linear assembly of the tangent stiffness matrix can substantially improve the performance, in particular, if only a small part of the domain is deformed. To switch between linear and non-linear assembly of an elementary stiffness matrix a criterion based on the monitoring of the displacement gradient (3.22) is used

$$\begin{aligned}
&\textbf{if } \max(|\boldsymbol{\nabla}\mathbf{u}|) < \epsilon_{\max} \quad \text{on } \Omega_i \subset \Omega \ : \\
&\qquad \textit{assemble} \quad C'_{ijkm} \approx C_{ijkm} \quad \text{on } \Omega_i \\
&\textbf{else} \ : \\
&\qquad \textit{assemble} \quad C'_{ijkm}(\boldsymbol{\nabla}\mathbf{u}^n) \quad \text{on } \Omega_i
\end{aligned}$$

In other words, if (3.22) indicates that the local linearization error is small, the non-linear terms in $C'_{ijkm}(\boldsymbol{\nabla}\mathbf{u}^n)$ can be neglected.

Adaptive mesh refinement. In order to solve the given boundary value problem via the finite element method, the domain of interest has to be discretized into subdomains. In accordance with Cea's lemma (3), the discretization error depends on the dimension of the finite element subspace, i.e. the number of nodal points and elements. On the other hand, the same parameters determine the dimension of the system of equations to be solved, and thus are directly related to the computational expenses. The key to the solution of this dilemma between the precision and the efficiency is the selective placement of nodal points, i.e. *adaptive mesh refinement*

There are several strategies for the adaptive meshing. Conventional adaptive schemes are based on the estimation of the local difference of the numerical solution obtained on the different order approximation spaces. For example, the error estimation for the solution approximated with linear basis function $\mathbf{u}_l$ consists in monitoring the difference $\|\mathbf{u}_q - \mathbf{u}_l\|$, where $\mathbf{u}_q$ is the solution obtained with quadratic basis functions. Efficient error estimators for the adaptive mesh re-

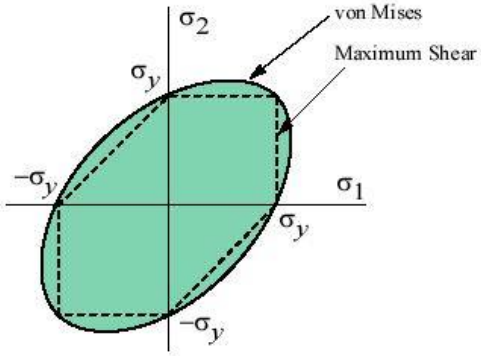

Figure 3.9: Von Mises and shear stress (Tresca) crack criteria (from [46, 83]).

fi nement based on hierarchical basis strategy are given in [31, 10]. Unfortunately, even simplifi ed hierarchical adaption schemes are quite expensive.

In fi nite element analysis of continuum mechanics problems, the goal of the adaptive meshing is intuitively evident: only large deformed regions have to be refi ned while the quiescent ones remain coarse meshed. The criteria of the "intensity" of the deformation known from fracture mechanics are based on the measurement of the deformation indicators such as the invariants of the stress or the strain tensor as for instance the *shear stress* or *Tresca criterion* [46, 83]

$$\max|\sigma_i - \sigma_j| \leq \sigma_c,\ i \neq j\,, \tag{3.105}$$

where $(\sigma_1, \sigma_2, \sigma_3)$ are the principal stresses and σ_c is a characteristic crack stress; or the *von Mises criterion*, see Figure 3.9

$$\frac{3}{2}(\sigma_1^2 + \sigma_2^2 + \sigma_3^2) \leq \sigma_c^2\,. \tag{3.106}$$

Since both the stress and the strain are the functions of the displacement gradient, a criterion based on (3.22) can be also used for the indication of large deformed regions. Subsequently, the solution on the refi ned mesh $\mathbf{u}_r$ have to be compared with the previously obtained one on the coarse mesh $\mathbf{u}_c$. The break condition is given by

$$\frac{\|\mathbf{u}_r - \mathbf{u}_c\|}{\|\mathbf{u}_c\|} \ll 1\,, \tag{3.107}$$

i.e. if the last refi nement is not followed by the signifi cant improvement of the solution. In order to be able to detect local differences corresponding to small regions, the norm $\|\cdot\|$ can be computed over the nodal points of the coarse mesh that belong to refi ned elements of these regions.

After the elements are marked for the refinement, edges and triangles of the corresponding tetrahedron have to be split as it is shown in Figure 3.10. Different refinements of tetrahedral elements are used to achieve a regular triangulation, that is the elements are allowed to intersect only by edges or triangles. Uncompleted refinements with node-edge or node-triangle intersections are not allowed.

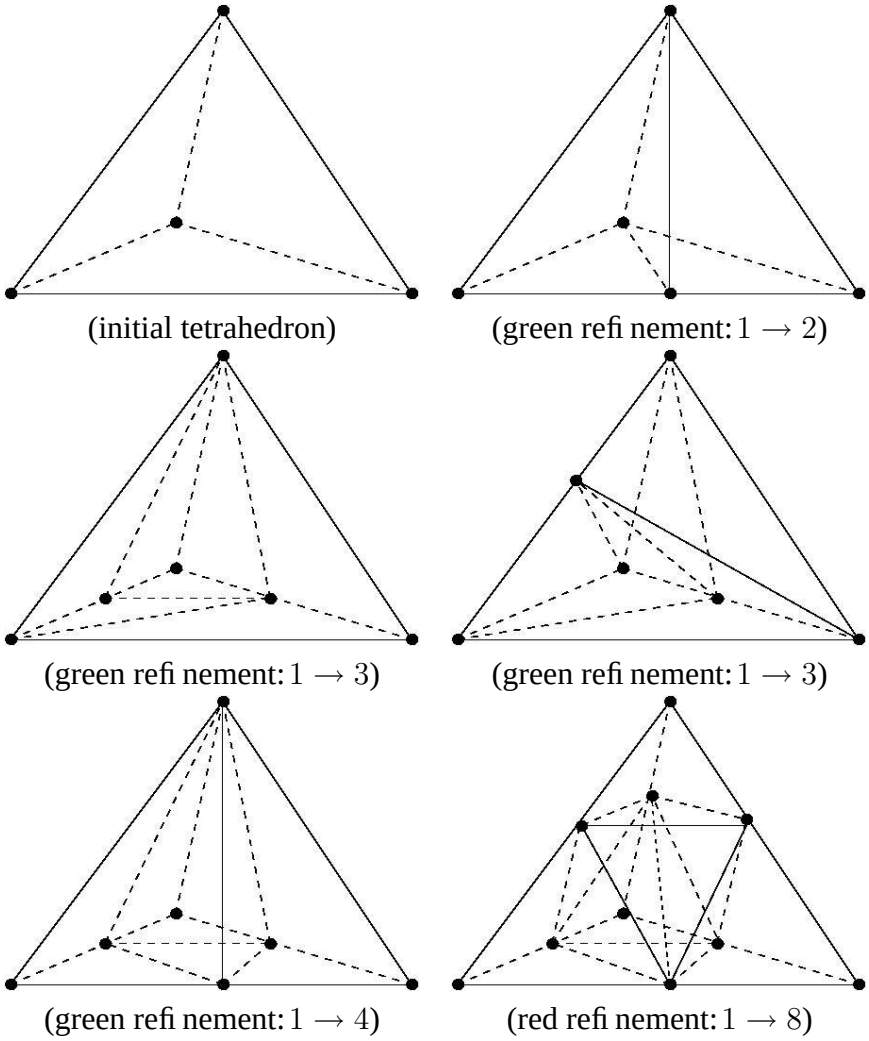

Figure 3.10: Tetrahedron refinement strategies (from [36]).